Environmental Science Advances

ROYAL SOCIETY OF CHEMISTRY

PAPER

View Article Online
View Journal | View Issue



Cite this: *Environ. Sci.: Adv.*, 2026, **5**, 510

# Process intensification by resonant vibratory mixing for samarium–cobalt magnet leaching with deep eutectic solvents

Zainab Nasrullah, *[a] Frank Agyemang, [a] Mehran Saddat [a] and Richard LaDouceur[b]

Due to limited primary resources and to fulfil the demand for renewable energy in the automobile industry, defence applications, and other high-tech applications, recycling rare earth elements (REEs) and other critical elements from their secondary resources is imperative. Rigorous research and development for viable extraction and separation of REEs and other critical elements has resulted from this need. Previously, Sm–Co recycling has been done using pyrometallurgy, physical separation, and hydrometallurgy, all of which have energy, cost, time, and environmental limitations. Chemical leaching has successfully recovered and separated Sm–Co but has limitations associated with slow mass transfer and leaching kinetics, especially using viscous lixiviants, and there is a need to intensify the process for efficiency. Additionally, environmental impact is high due to extensive use of toxic, corrosive, non-selective, and expensive reagents. In this research, chemical leaching of Sm–Co was performed using Deep Eutectic Solvents (DESs), a new class of solvents under solvometallurgy. Four different DESs were studied, which are green, non-toxic, biodegradable, cheap, and selective. To enhance the mass transfer and reduce leaching time, resonant vibratory mixing (RVM) was tested. RVM intensifies mixing by establishing low energy conditions through vessel resonance, improving kinetics. Four DES combinations were prepared: choline chloride and tetrabutylammonium chloride, with oxalic acid, urea, and ethylene glycol at 80 °C. Chemical leaching of Sm–Co was performed using factors of time (hours), temperature (°C), and combination of DESs. Post-leaching, the samples were process intensified using RVM (time, intensity, and four DESs). Filtered aliquots were analysed with ICP-OES. Oxaline was the most selective DES, achieving 82% Co conversion after 2 hours of leaching and 30 minutes of RVM at 80 °C. A preliminary kinetic study determined the activation energy barrier and showed an increase in conversion (%) for both Co and Sm. 93.4% Co and 5.3% Sm conversions were achieved with only 5 hours of leaching at 90 °C, and after process intensification with RVM, conversions of 97% Co and 9.3% Sm were achieved.

Received 22nd August 2025
Accepted 17th November 2025

DOI: 10.1039/d5va00283d

rsc.li/esadvances



### Environmental significance

The recovery of samarium (Sm) and cobalt (Co) is essential to support clean energy technologies and reduce dependence on the primary resources of these critical REEs. Traditional Sm–Co magnet recycling methods are energy-intensive, time-consuming, and not environmentally benign. This study presents a green and efficient leaching process using DESs, which are biodegradable, non-toxic, and selective. This process, when combined with resonant vibratory mixing (RVM) technology, can enhance slow mass transfer and kinetics. In this research project, intensifying leaching under low-energy conditions resulted in selective recovery of Co in shorter times using green DES reagents. This process provides a greener, safer, and more efficient alternative to conventional methods, advancing the sustainable solvometallurgical recycling of Sm–Co magnets in line with circular economy principles.

## 1 Introduction

Together with yttrium (Y), scandium (Sc), and lanthanides, rare earth elements (REEs) are a collection of 17 chemically related elements.[1] Due to their distinctive physical and chemical characteristics, rare earth elements (REEs) are valuable resources that are necessary for a wide range of modern technological applications, including metallurgy, machine building, radio electronics, instrument engineering, nuclear engineering, and manufacturing.[1–3] Many nations' economic growth and national security depend on the reliable supply and durability of these vital resources.[4] Rare earth element availability is currently less than demand,[5,6] with imports from China

[a]*Department of Metallurgical and Materials Engineering, Montana Technological University, Butte, Montana, USA. E-mail: znasrullah@mtech.edu*
[b]*Department of Mechanical Engineering, Montana Technological University, Butte, Montana, USA*

frequently accounting for a large portion of the supply, so most industrialized nations require imports from China[7,8]. The United States is seeking to expand domestic production and recover rare earth elements (REs) from various sources to reduce supply chain vulnerability, given the significance of these minerals in technological and economic advancement.[4,9]

It is challenging to mine REEs since they are frequently found in dilute concentrations.[5] The extraction and separation of REEs from their complex ores are complicated due to their unique physical and chemical properties, making them scarce in the market.[1] The recovery of REEs involves traditional pyro- or hydrometallurgical processes, such as solvent extraction.[10] The pyrometallurgical method suffers from environmental concerns such as gaseous emissions, while the traditional hydrometallurgical process involves using dilute and strong acids to dissolve REEs, which results in the evolution of hydrogen gas.[11,12] The recovery and separation of individual elements from complex REE systems suffer from high energy demands as they require complex energy-consuming solutions using many hazardous chemicals that negatively impact the environment.[5] In response to REE scarcity and potential supply risk, recent research has focused on improving recovery and separation techniques and developing recycling approaches for secondary resources like mine tailings and electronic waste as alternative sources to natural ores.[13,14] The evolution of recycling processes as a secondary source for REEs has seen the majority of rare-earth magnet recycling research concentrated on NdFeB magnet recycling,[15–17] with little attention to Sm–Co magnet recycling.[7] However, the recycling of Sm–Co magnets will not only be a secondary source for samarium but also cobalt, a critical metal that is economically very important for the steel industry[14,18] due to its unique resistance to oxidation and its usage in cathode materials for lithium-ion batteries, which is very crucial to the transition to electric vehicles.[14]

Neodymium and samarium, two of the least abundant of the REEs, are the foundational elements for making powerful permanent magnets.[19] The most prevalent REE magnets are Nd–Fe–B magnets.[20] Since neodymium–iron–boron (NdFeB) magnets primarily replaced Sm–Co magnets after 1985,[13] the Sm–Co magnet market share is currently less than 2% in the permanent magnet segment.[13,14] Nonetheless, new applications in consumer electronics, automotive and medical technology, aerospace, and military equipment are driving growth in the global market for Sm–Co magnets. Due to their greater optimal operating temperature (250–350 °C) than that of Nd–Fe–B magnets (60–220 °C), Sm–Co magnets are still valued for their capacity to operate at elevated temperatures. They are frequently utilized in the aviation industry.[14,21] Samarium is utilized in the filter glass of Nd:YAG (neodymium:yttrium–aluminium–garnet) solid-state lasers to encircle the laser rod and increase efficiency by collecting stray emissions due to its narrow spectral absorption band.[11] Samarium can be used in coatings and capacitors at microwave frequencies because it forms stable titanate compounds with beneficial dielectric characteristics.[11] Cobalt and samarium can be obtained from end-of-life Sm–Co magnets as valuable secondary sources.[14]

With the growing trend toward a circular economy that aims to balance sustainability, efficiency, and environmental impacts, this research is focused on recycling Sm–Co magnets using green (ionometallurgy), innovative, and novel extraction pathways. Specifically, it involves the use of Deep Eutectic Solvents (DESs) for leaching and novel Resonance Vibratory Mixing (RVM) to intensify the leaching process.

DESs are systems formed from eutectic mixtures of Lewis or Brønsted acids and bases, which can contain a variety of anionic and cationic species.[22] The eutectic combinations have melting points lower than their components, giving a room-temperature ionic liquid,[23] meaning they are liquid at temperatures lower than 150 °C, but most are between 25 and 70 °C.[24] The advantages of DESs over conventional hydrometallurgical reagents are that they are environmentally benign or have minimal risk and environmental impacts, are readily available in larger quantities, are cost-efficient and chemically stable to allow prolonged reuse, and do selective leaching.[10,25] A DES is typically created by combining a quaternary ammonium salt with metal salts or a hydrogen bond donor (HBD) that can form a complex with the quaternary ammonium salt's halide anion. DESs are defined using the general formula $Cat^+X^-zY$ where $Cat^+$ is an ammonium, phosphonium, or sulfonium cation, X is a Lewis base, generally a halide anion with choline chloride [ChCl, $HOC_2H_4N^+(CH_3)_3Cl$)] widely used as a halide salt, and Y is a Brønsted acid while $z$ refers to the number of Y molecules that interact with the anion.[22] Although DESs differ slightly from traditional ionic liquids in that they are mixtures rather than isolated salt compounds, their anhydrous nature and shared characteristics make them suitable for metal recovery. There are four types of DES systems. Table 1 shows the classification of DESs formed based on the nature of the complexing agent used.

The type III DESs namely Reline (choline chloride 1 : 2 urea), ethaline (choline chloride 1 : 2 ethylene glycol), oxaline (choline chloride 1 : 1 oxalic acid) and EG : TBAC (ethylene glycol 2 : 1 tetrabutylammonium chloride) were used for this research due to advantages over the other types of DESs that make them useful for large-scale industrial processes. Some of their advantages include the ability to solvate a wide range of transition metal species, including chlorides,[26] oxides,[27] and rare earth elements, ease of preparation, relative unreactivity with water, relatively low cost, and their biodegradable nature.[28–30]

Typically, one of the significant drawbacks of leaching is slow kinetics.[31] DESs have higher viscosity than aqueous solvents,[10,32] and since chemical reactions have slow kinetics in viscous liquids,[32] the leaching kinetics may be significantly affected. Water can be added to DESs to reduce their viscosity, but adding water, or too much water, can change their physicochemical properties.[32,33] Increasing the temperature is another way to reduce the viscosity,[18,32] but this may increase the cost of operation on an industrial scale. For this reason, RVM can be utilized to intensify the leaching process. RVM uses resonant vibration to increase the rate of homogeneity through motion and improve contact time and thus mass transfer.[34] RVM mixers create and regulate vertical motion by consuming minimal power by operating the driving force and reactor at resonance, which moves and vibrates the resonator plate,

Table 1 The general formula for the classification of deep eutectic solvents. These are classified based on the nature of the complexing agent used. Type I is an analogous combination between the metal chloride and quaternary ammonium salts, type II is based on the combination of hydrated metal chloride and salt, type III is based on the combination of transition metal and salt, and type IV is based on a wide range of transition metals combined with inorganic cations to form a eutectic[26]

| Type | General formula | Terms |
|---|---|---|
| Type I | $Cat^{+}X_z^{-}MCl_x$ | M = Zn, Sn, Fe, Al, Ga |
| Type II | $Cat^{+}X_z^{-}MCl_{xy}H_2O$ | M = Cr, Co, Cu, Ni, Fe |
| Type III | $Cat^{+}X_z^{-}RZ$ | Z = $CONH_2$, COOH, OH |
| Type IV | $MCl_x + RZ = MCl^{*}_{x-1}RZ + MCl_{x-1}$ | M = Al, Zn and Z = $CONH_2$, OH |

affecting the mixing vessel's contents. RVM systems are particularly effective because they balance frequency and displacement, unlike other mixing technologies like ultrasonics, which function at very high frequencies but only generate displacement within a small area immediately surrounding the frequency-generating probe.[35] The intensification due to RVM will shorten leaching time by increasing leaching kinetics and overall leaching efficiency or recovery, thereby cutting operational costs. The intensification process accelerates the diffusion process by causing a change in the hydrodynamic situation in the interfacial layer and the adjacent layers of liquids due to the supply of additional energy and the updating of the phase contact surface.[36]

# 2 Materials and methods

## 2.1 Materials

The chemicals used in the present work were of analytical grade. The specifications of the chemicals are as follows: choline chloride ($C_5H_{14}NOCl$), tetrabutylammonium chloride ($C_{16}H_{36}C_1N$), oxalic acid ($C_2H_2O_4$), ethylene glycol ($(CH_2OH)_2$), and urea ($CO(NH_2)_2$). These were sourced from Thermo Scientific with a purity of <98.99% and were used as received for research purposes. Sm–Co magnets were provided by Integrated Magnets Inc., Culver City, California, USA. A ball mill (TITAN Model) and a mortar and pestle were utilized to reduce the size of the Sm–Co magnets. To obtain a representative sample from the bulk of Sm–Co magnets, ASTM standard D6323-98 was followed. Coning, quartering, and a Jones riffle were employed for homogenization and sampling. Sieves (W.S. Tyler) of 40, 60, and 200 mesh numbers were used for sieving. A magnetic stirrer hot plate (IKA RET control VISC S000) and resonant vibratory mixer (Resodyn LabRAM II) were utilized for the leaching and mixing experiments.

## 2.2 Characterization

The surface morphology of the feed sample and the solid residue of Sm–Co was determined using SEM (TESCAN TIMA). The weight composition (%) of the feed sample was determined using EDX (EDAX Z4-i7+ Analyzer), as shown in Table 2.

Table 2 Metal content weight composition (%) in the Sm–Co magnet material determined using energy dispersive X-ray spectroscopy (EDS)

| Element | Sm | Co | Fe | Cu |
|---|---|---|---|---|
| wt% | 20.4 ± 5.9 | 52.6 ± 3.2 | 14.8 ± 3.8 | 3.45 ± 13.2 |

## 2.3 Experimental procedure

The research methodology is shown in Fig. 1. After feed characterization, four DES combinations were prepared, and Sm–Co chemical leaching was performed. Afterward, the chemical leaching solution was divided into two aliquots: the first aliquot was analysed by ICP-OES, and the second was mixed using RVM technology to assess the enhancement of leaching kinetics.

**2.3.1 Preparation of DESs and their properties.** The DESs were prepared by mixing a molar ratio of hydrogen bond donor (HBD) and hydrogen bond acceptor (HBA). The molar ratio of HBA and HBD was 1 : 1 for ChCl : oxalic acid, 1 : 2 for ChCl : urea and ChCl : ethylene glycol, and 1 : 2 for TBAC : ethylene glycol, respectively. The eutectic mixture was heated using a hot plate to a temperature of 80 °C and stirred at 400 rpm for 1 to 4 hours until a homogeneous and transparent solution was formed. The DESs were stored in glass bottles in an oven at 50 °C for leaching experiments. The combinations of DESs in Table 3 were used as a lixiviant for the chemical leaching of Sm–Co magnets.

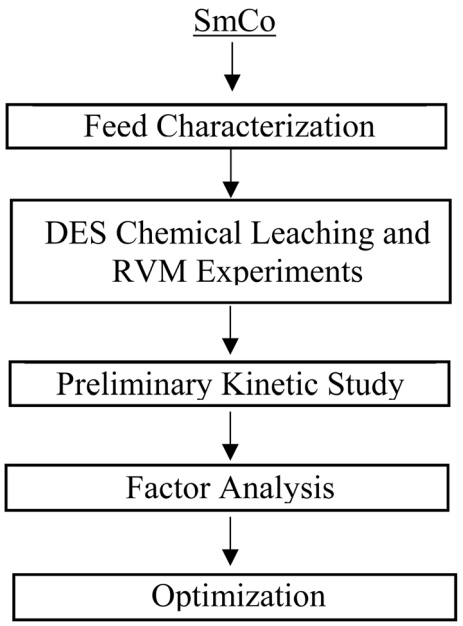


Fig. 1 A flowchart for methodology was incorporated for Sm–Co chemical leaching and process intensification with resonant vibratory mixing.

Table 3 Four different combinations of deep eutectic solvents (DESs) based on two hydrogen bond donors (HBDs): choline chloride and tetra-butyl ammonium chloride. Three organic compounds were used, which function as hydrogen bond acceptors (HBAs): urea, ethylene glycol, and oxalic acid. Based on varied mixing ratios of 1 : 1 and 1 : 2 of HBD : HBA, four unique combinations of DESs were obtained

| Organic acid (HBD) | Salt (HBA) | Combination name |
|---|---|---|
| Oxalic acid | Choline chloride | Oxaline |
| Ethylene glycol | Choline chloride | Ethaline |
| Urea | Choline chloride | Reline |
| Ethylene glycol | Tetra butyl ammonium chloride | EG–TBAC |

**2.3.2 Chemical leaching of Sm–Co.** For the chemical leaching experiments, an experimental design (DOE) was used, which had 52 runs based on the factors of leaching time (hours), temperature (°C), and a combination of DESs using response surface methodology and a face-centred central composite design found in Table S1. Stat-Ease Design Expert 13 was used to generate and analyse the DOE. The low and high levels for the leaching factors were 0.59–2 hours for leaching time, 60–90 °C for temperature, and four DES combinations. Leaching experiments were performed as a batch process in a glass reactor using the prepared DES combinations and were mechanically stirred at 400 rpm and at a leaching time defined by Design Expert in Table 4.

Leaching experiments were performed as a batch process in a glass reactor using the prepared DES combinations and were mechanically stirred at 400 rpm and at a leaching time range defined by Design Xpert. The tests were carried out with a solid-to-liquid ratio of 1 : 5 (0.2 g of sample with a size fraction of +250 μm/−425 μm was taken, and 10 mL of prepared DESs was added). The temperatures at which the test was carried out were 60 °C, 70 °C, 80 °C, 90 °C. After leaching, 2 mL of the pregnant solution was withdrawn, filtered, diluted with nitric acid (5%), and analysed by ICP-OES. 2 mL of the lixiviant was added to the leaching solution to compensate for the 2 mL of the pregnant solution that was periodically taken for ICP-OES analysis and then used in subsequent RVM experiments.

Table 4 shows the leaching parameters for the leaching experiment. The conversion of Sm–Co concentrations in the sample was calculated according to eqn (1):

$$X\% = \frac{C \times \mathrm{DF}}{C_0} \times 100 \quad (1)$$

where $X$ is the conversion, DF is the dilution factor, $C$ is the concentration of REEs in the leachate (mg $L^{-1}$), and $C_0$ is the maximum amount of REEs that can be leached out (mg $L^{-1}$).

**2.3.3 Resonant vibratory mixing experiments.** For the RVM experiments, an experimental design (DOE) was used, which had 52 runs based on the factors of time (minutes), intensity (%), and a combination of DESs using response surface methodology and a face-centred central composite design found in Table S2. Stat-Ease Design Expert 13 was used to generate and analyse the DOE. The low and high levels for the time factor were 1–30 minutes, intensity (%), 10–70%, and DES combinations in Table 5 were used.

For each run of RVM experiments, 11 mL of an aliquot was taken. The filtered 3 mL aliquot was pipetted and stored in an oven at 50 °C for quantitative analysis using ICP-OES.

**2.3.4 Preliminary kinetic study experiments.** A preliminary kinetic study using the Arrhenius equation ($k = Ae^{-E_a/RT}$) was conducted to evaluate the effect of temperature on leaching conversion (%) of Co and Sm and to determine the RVM's role in enhancing the leaching kinetics by calculating the change in activation energy barriers for Sm and Co with oxaline DES for both chemical leaching and RVM. To determine the activation energy of the leaching reactions, the data of the leaching experiments were fitted to a polynomial curve to determine the initial rate. Then, the Arrhenius equations were applied according to eqn (2) and (3):[37]

$$k = A\, e^{\frac{-E_a}{RT}} \quad (2)$$

$$\ln k = \ln A + \frac{-E_a}{RT} \quad (3)$$

Accordingly, a plot of $\ln k$ against $1/T$ gives a slope $= -E_a/R$, where $A$ is the pre-exponential factor, $R$ is the universal gas constant (8.314 J $mol^{-1}$ $K^{-1}$), $T$ is the temperature expressed in kelvin, and $E_a$ is the apparent activation energy of the reaction. The study was completed using the varying conditions for chemical leaching, as shown in Table S3.

To determine the activation energy by incorporating RVM, the study was completed under the same leaching conditions as shown in Table S3, and the conditions of RVM were varied, as shown in Table S4.

Table 4 The factors and range of values selected for chemical leaching of Sm–Co magnets with four different combinations of deep eutectic solvents

| Factors | Range and combinations |
|---|---|
| A: time/hours | 0.59–2 |
| B: temperature/°C | 60–90 |
| C: DES combinations | Oxaline, Ethaline, Reline, EG–TBAC |

Table 5 The factors and range of values selected for process intensification using resonant vibratory mixing technology for Sm–Co magnets after chemical leaching

| Factors | Range and combinations |
|---|---|
| Time/minutes | 1–30 |
| Intensity/% | 1–70 |
| DES combinations | Reline, Oxaline, Ethaline, EG–TBAC |

# 3 Results and discussion

A discussion of the results of all the experiments undertaken for this research is presented in this section. These will include the Sm–Co leaching in different DESs (ethaline, Reline, oxaline, and EG–TBAC), the effect of time, and RVM intensification. It will include the ANOVA, Fit Statistics, the leaching and RVM activation energy barrier study, and solid residue analysis using SEM and EDS analysis.

## 3.1 Chemical leaching using four deep eutectic solvent combinations

The results for Sm and Co conversion (%) in different DES media, which are found in detail in Table S1, are presented in Fig. 2. The highest conversion for Co was obtained in oxaline leaching. Oxaline leaching achieved 82% conversion; ethaline, Reline, and EG–TBAC showed lower conversion. The Co conversion order in the leaching media is oxaline > Reline > EG–TBAC > ethaline. For the Sm conversion, the order is ethaline > Reline > EG–TBAC > oxaline. The pH of the studied DES is in the following order: oxaline (2.037)[38] > ethaline (4–4.4)[38] > EG–TBAC (7.5–9.10)[39] > Reline (10.8).[29] This reason supports why the conversion of Sm is higher in ethaline, because ethaline is a weak acid, and REE reacts slowly in strong bases. For oxaline and ethaline, despite oxaline's higher acidity, oxaline promotes the formation of insoluble samarium-oxalate complexes that passivate the surface and inhibit leaching, whereas cobalt forms more soluble oxalate species, enabling higher dissolution efficiency.[40,41]

Oxaline DES leaching has the highest selectivity to Co(II) over Sm(III) ions. The Sm dissolution is relatively low, with less than 10% conversion, compared to the high Co conversion of approximately 65% after 2 hours. It can also be seen that time significantly affects the Sm and Co dissolution process. It is observed that, as the time continued to increase, the leaching efficiency did not plateau. This indicates that a further increase in time for the leaching process will increase the Co conversion rate. Oxaline is an acidic DES,[38] and the low conversion of Sm in oxaline leaching can be attributed to the slower reaction rates of REEs with organic acids.[11] The low conversion of Sm could be due to the presence of a protective layer on the surface, which prevented the contact of oxaline with the metal, as previously reported.[42]

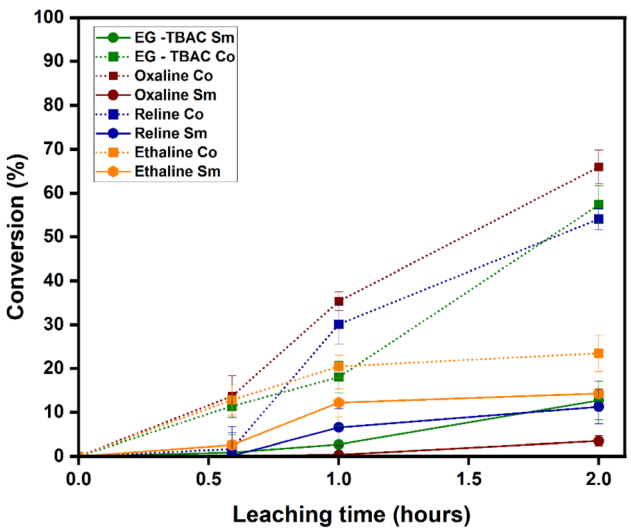


Fig. 2 Comparison of Sm and Co conversion in four DES media: EG–TBAC, Ethaline, Oxaline, and Reline at 0.59, 1, and 2 hours. For each experiment, these conditions were kept constant: 80 °C, 400 rpm stirring speed, and 55 : 1 liquid to solid ratio.

Reline DES leaching conversion is not proportional to the Co conversion. As can be seen, the conversion of Sm is very low at about 10%, and the Co conversion is higher at about 55%, indicating a high selectivity of Reline to Co over Sm. Also, the conversion for both Sm and Co increases with increasing time. Rare earth metals react slowly with strong bases[11] because they form a passive, insoluble hydroxide layer on their surfaces,[43] and since Reline is a mildly strong alkaline DES,[29] the low conversion of Sm in Reline can be attributed to it. The high conversion of Co in Reline results from its alkaline nature, which forms a soluble anionic or complex species instead of insoluble hydroxide,[44] which passivates the surface layer and reduces leaching efficiency.

Ethaline DES leaching conversion for Sm dissolution is relatively low, at about 14%, compared to the Co conversion of about 24% after 2 hours. The low recovery of Sm and Co in ethaline can be attributed to the formation of a passivating layer around the metal's surfaces.[45,46] Although ethaline is a moderate acid, it is not a strong complexation agent for Sm and has a low proton activity to break down the passivating layer. It can be seen from the result that ethaline does not show high selectivity for either Co or Sm over the other, even though the conversion is not proportional for both Co and Sm. It can also be seen that time significantly affects the Sm and Co dissolution process. The difference between the Co and Sm conversion is low compared to the results obtained for oxaline and Reline. Ethaline is a weak acid.[38] Since Co dissolves slowly in a weak acid, this could be why the conversion of Co is lower in ethaline than in oxaline, which is a strong acid. In weak acids, Co typically develops a protective oxide or hydroxide layer that passivates it and prevents further reaction with the acid. Since the hydrogen ion concentration in the weak acid is too low to effectively break this passivation layer, the dissolution proceeds slowly.[47,48]

EG–TBAC DES leaching shows that the Sm conversion is not proportional to the Co conversion. As can be seen, the conversion of Sm is low at about 12%, and the Co conversion is higher at about 60%, indicating a high selectivity of EG–TBAC to Co over Sm. Also, the conversion for both Sm and Co increases with increasing time. Rare earth metals react, but slowly, with strong bases,[11] and since EG–TBAC is a strong alkaline,[49] the low conversion of Sm can be attributed to it.

## 3.2 Chemical leaching with RVM using two DESs

The results for Sm and Co conversions (%) after RVM intensification can be found in Table S2. This section focuses only on oxaline and Reline DESs due to the highest achieved selectivity for Co over Sm over the other DES combinations used for this

research. Sm and Co conversions in oxaline and Reline DES leaching are compared to the conversions of Sm and Co after intensifying the leaching process with RVM.

**3.2.1 Oxaline.** From Fig. 3, Sm and Co conversions increased with the RVM intensification after 30 minutes using oxaline DES. Sm and Co's dissolution rate did not plateau, indicating that higher conversions can be attained by increasing the intensification time. The increase in conversion after the intensification can be attributed to the RVM, which speeds up the liquid's motion and intensifies interfacial mass transfer.[50] This liquid motion increases the area around the interface,[51,52] thereby enhancing the diffusion process.[36]

**3.2.2 Reline.** From Fig. 4, Sm and Co conversions increased after RVM intensification. Sm and Co's dissolution rate did not decrease after 30 minutes, indicating that the intensification time can be increased further to achieve higher conversions using Reline. The increase in conversion after the intensification can be attributed to the change in the interfacial hydrodynamic layer caused by the resonant vibration of the RVM,[36] thereby accelerating the mass transfer process.[36]

### 3.3 Analysis of variance and fit statistics

The results for face-centered central composite experimental design comprising 52 runs for Co and Sm leaching and RVM are found in Tables S1 and S2, respectively. Tables S5 and S6 present the ANOVA and fit statistics for co-leaching and RVM. Similarly, Tables S7 and S8 present the results for Sm leaching and RVM.

**3.3.1 Cobalt.** Table S5 for Co leaching demonstrates the significance of the models. The adjusted $R^2$ of 0.99 and the predicted $R^2$ of 0.96 are still close, differing only by approximately 0.01. The model with the individual main effects of temperature, leaching time, and DES combinations presented

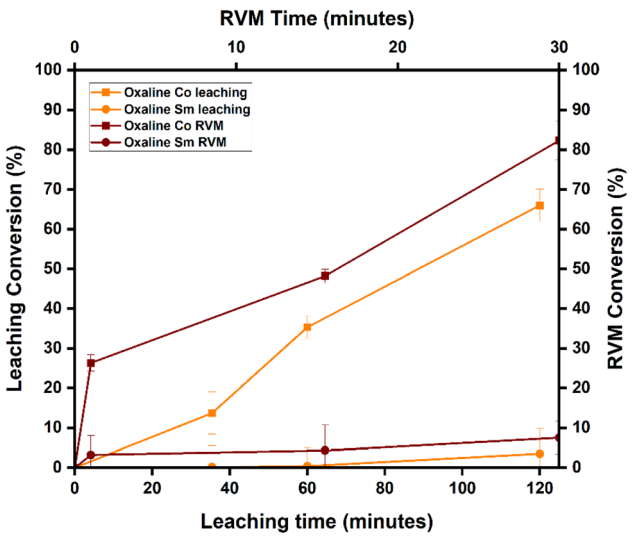


Fig. 3 Samarium (Sm) and cobalt (Co) dissolution at 80 °C from the Sm–Co magnet in Oxaline leaching for 0.59, 1, and 2 hours and RVM intensification at 70 g intensity (%) for 1, 15, and 30 minutes. For each experiment, these conditions were kept constant: 400 rpm stirring speed and 55 : 1 liquid to solid ratio.

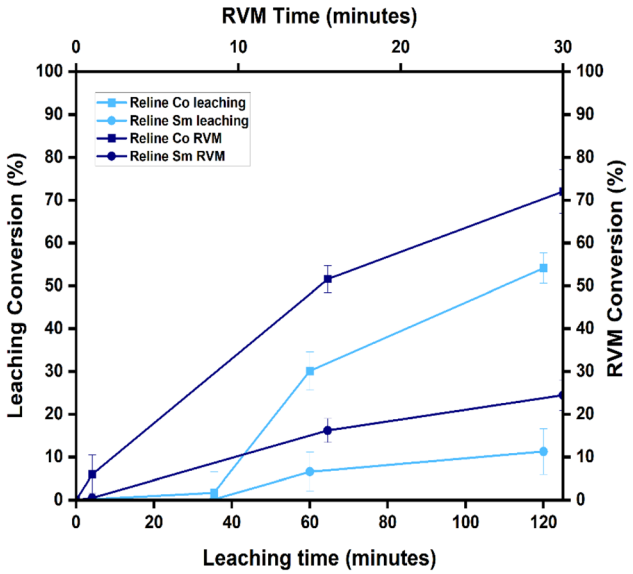


Fig. 4 Samarium (Sm) and cobalt (Co) dissolution at 80 °C from Sm–Co magnet in Reline leaching for 0.59, 1, and 2 hours and RVM intensification at 70 g intensity (%) for 1, 15, and 30 minutes. For each experiment, these conditions were kept constant: 400 rpm stirring speed and 55 : 1 liquid to solid ratio.

significantly low $p$-values (<0.0001), indicating a significant impact on Co conversion (%). For the adeq. precision, which evaluates the signal-to-noise, the value obtained was 43.89 (a value greater than 4 is desirable), indicating a strong signal. The higher number of experiments could have caused the lack of fit. The models' ability to predict future values in the design space is also supported by statistical parameters, such as predicted $R^2$ and CV%.

Table S6 for Co RVM demonstrates the significance of the developed models. With a small difference well below 0.01 and a predicted $R^2$ of 0.97, which closely matches the adjusted $R^2$ of 0.99. The model's primary effects (temperature, leaching time, resonant vibratory mixing intensity, and DES combinations) present low $p$-values (<0.0001), indicating their significant influence on Co conversion (%). A robust signal of 60.60 is indicated by the adeq. precision. The high number of 52 experimental runs, which can more sensitively reveal systematic deviations, may be the cause of the model's notable lack of fit. Furthermore, the model's predictive ability and dependability in examining the design space for future Co leaching experiments are further supported by the satisfactory CV% and predicted $R^2$ values.

**3.3.2 Samarium.** Table S7 for Sm leaching demonstrated the models' significance. With a difference of less than 0.04, the adjusted $R^2$ of 0.95 and the predicted $R^2$ of 0.91 are nearly identical. Both the model and its individual main effects (temperature, leaching time, and DES combinations) demonstrated low $p$-values (<0.0001), indicating that they had a significant impact on Sm conversion (%). The quadratic term ($A^2$) and interaction terms ($AB$, $AC$, and $BC$) also exhibit significant $p$-values (<0.0001 to 0.0008), confirming their inclusion in the model. A sufficient signal is indicated by the adeq. precision

of 43.89. The larger number of runs (52 experiments), which reveals systematic deviations, may be the cause of the model's notable lack of fit. The model's capacity to predict future values and navigate the design space is confirmed by the statistical parameters, such as predicted $R^2$ and CV%, which likewise fall within a satisfactory range.

Table S8 for Sm RVM demonstrates the significance of the developed model, as reflected by the predicted $R^2$ of 0.95, closely matching the adjusted $R^2$ of 0.97, with a difference well below 0.02. The model and its main effects (temperature, leaching time, RVM intensity, and DES combinations) present low *p*-values (<0.0001), indicating that they have a significant influence on Sm conversion (%) after incorporating RVM. Notably, RVM intensity (%) has the strongest impact on the leaching process, as evidenced by its highest *F*-value of 353.00. The roles of the interaction terms *AE*, *BD*, and *BE* in the model are further validated by their significant contributions ($p < 0.05$). The robust signal is demonstrated by the adeq. precision of 50.30. The high number of experimental runs (52 experiments) may be the cause of the model's notable lack of fit. The model's predictive ability and dependability in examining the design space for Sm leaching experiments employing RVM technology are further supported by the high $R^2$ of 0.98 and the satisfactory CV%.

### 3.4 Effect of temperature on Co and Sm leaching in oxaline and RVM

The effect of leaching under varying time and temperature (°C) conditions on Co conversion (%) is shown in Fig. 5(a). Co conversion increases proportionally with time (1–5 h) and temperature (60–90 °C), reaching a maximum of 93.35% after 5 hours at 90 °C. This matches previous findings, where Co dissolves quickly in DES-enriched acidic media due to weak Sm–Co bonding.[46–48] As a transition metal with variable oxidation states (+2, +3), Co forms stable complexes and preferentially leaches into solution.[46–48]

Fig. 5(b) shows Co conversion (%) with time and temperature after RVM introduction. Similar to previous results, Co conversion rises with increased time and temperature, peaking at 97% after 5 hours at 90 °C with 30 minutes of RVM. Co's higher conversion reflects its ability to form stable oxaline DES complexes $[Co(DES)^{n+}]$.[53] RVM improves DES access to Co by reducing diffusion barriers like pore blocking or stagnant layers,[51,52] enhancing Co leaching efficiency from 93% to 97%. RVM proves effective in mass transfer and near-complete Co leaching.

Under the same conditions, Sm conversion (%) is shown in Fig. 5(c). It also increases with time and temperature, but at a slower rate, reaching a maximum of 5.3% after 5 hours at 90 °C. This aligns with past studies: Sm forms stable oxides ($Sm_2O_3$) and resists leaching unless pretreated.[54] Compared to Co, which forms $Co_3O_4$ and leaches more readily, Sm dissolves slowly in DESs due to poor complex stability and weak ligand field stabilization energy (LFSE) from its shielded 4f orbital.[46,48]

Fig. 5(d) shows Sm conversion (%) after RVM use. Even with RVM, Sm reaches only 9% conversion under the same time and temperature conditions. This reflects Sm's inherent limitations as a REE with a 3+ oxidation state and large ionic radius, hindering ligand coordination and resulting in a slower leaching rate compared to Co.

### 3.5 Activation energy barrier

The activation energy from the dissolution of Sm and Co was determined using Arrhenius law for Co and Sm in oxaline leaching and RVM.

**3.5.1 Co leaching *vs.* RVM.** In Fig. 6(a), the Arrhenius relationship between $1000K/T$ and $\ln K$ was plotted, and the activation energy for Co was determined to be 27.10 kJ mol$^{-1}$ with chemical leaching, which reveals that Co extraction is controlled by a diffusion-limited mixed-controlled reaction. The low activation energy calculated indicates that minimum energy is required for the chemical reaction to take place, which can be attributed to the high Co conversion (%). The mixed-controlled reactions also may have contributed to the high Co separation and extraction and suggest that it is less thermally dependent. This is consistent with the past studies on Co leaching.[47,48]

In Fig. 6(b), the activation energy was determined to be unchanged from the 27.10 kJ mol$^{-1}$ of chemical leaching, which reveals that RVM Co extraction is a mixed control reaction. Its low and unchanged $E_a$ value is an indication that RVM only plays an enhancement role in reducing the boundary layer resistance and optimizing the existing kinetics rather than altering the rate-limiting steps.

**3.5.2 Sm leaching *vs.* RVM.** The activation energy of Sm was calculated to be 65.74 kJ mol$^{-1}$ (Fig. 7(a)), which reveals that a chemical-controlled reaction controls Sm extraction. Sm's lower conversion (%) can be attributed to the high activation energy calculated as compared to the activation energy calculated for Co, indicating that more energy is required for the chemical reaction to take place. This suggests it is more thermally dependent. This minimal conversion (%) of Sm in the acidic enriched medium is consistent with the past studies on Sm leaching, where specialized chelating agents or pretreatments are used for higher conversion (%).[47,48]

In comparison to $Co^{3+}$ (3500–4000 kJ mol$^{-1}$), $Sm^{3+}$ also has a higher lattice energy (12 878 kJ mol$^{-1}$), contributing to Sm's rigid lattice structure and its ability to form highly stable metal oxide bonds.[49,50] The evident decrease in $E_a$ from 65.7 to 59.2 kJ mol$^{-1}$ after RVM introduction in Fig. 7(b) suggests that RVM partially alleviated diffusional limitations, and RVM vibrations likely enhanced the solvent penetration of oxaline DES for Sm. Despite RVM, Sm leaching resulted in a low conversion (%) of Sm, which reveals that Sm conversion (%) was limited by the intrinsic stability of Sm–O bonds, which need further harsh pretreatment, and RVM alone cannot overcome this thermodynamic behaviour.[51]

### 3.6 Solid residue analysis in oxaline

Since oxaline gave the best results for this research study, solid residue analysis was focused on the solid residue from the leaching in oxaline DES. For this analysis, SEM and EDX were used after the chemical leaching of Sm–Co with oxaline for conditions 1, 2, and 5 hours at 90 °C.

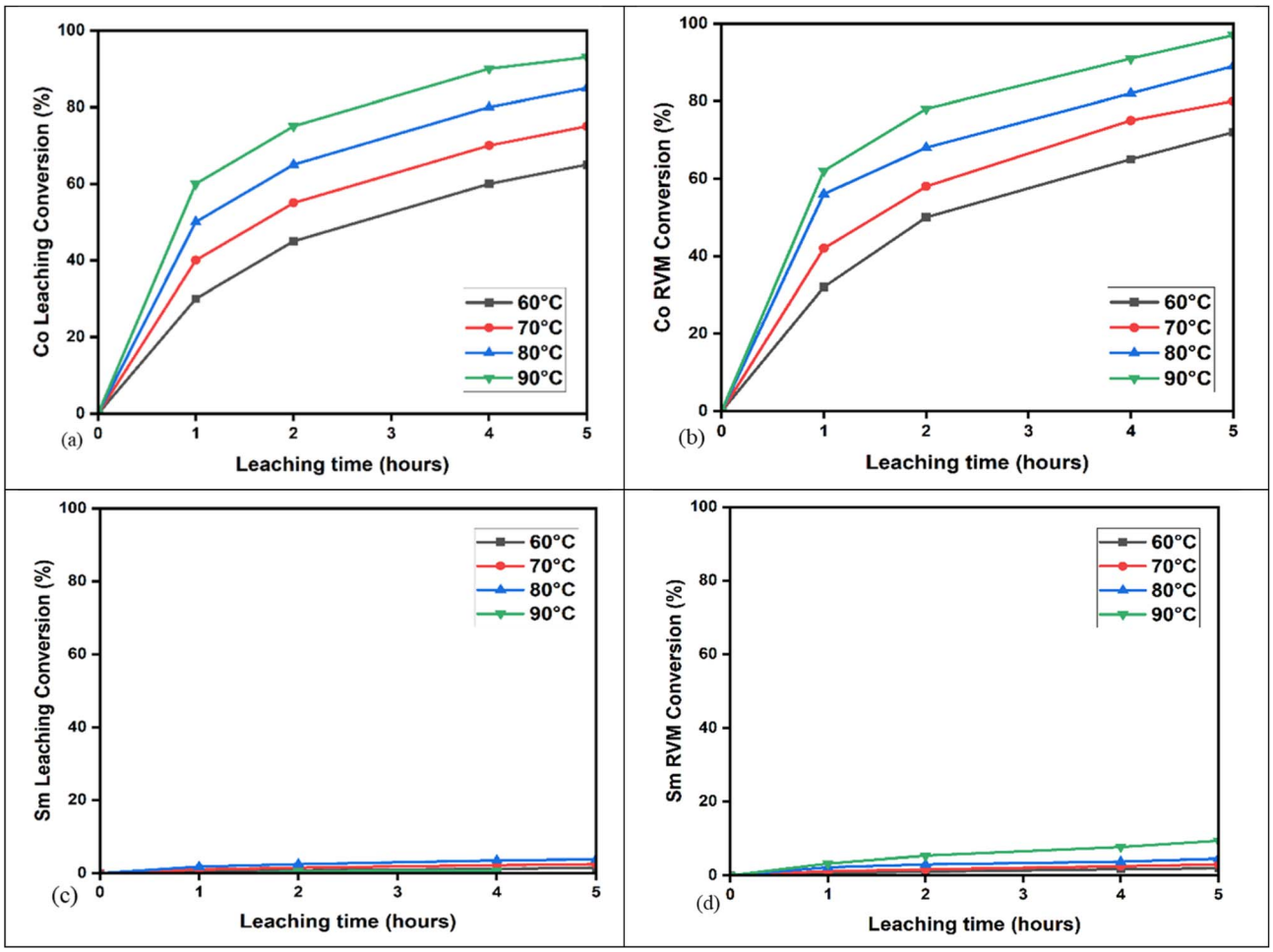


Fig. 5 Effect of varying temperatures of 60, 70, 80, and 90 °C and times of 1, 2, 4, and 5 hours on (a) Co leaching conversion (%). (b) Co RVM conversion (%). (c) Sm leaching conversion (%). (d) Sm RVM conversion (%). For each experiment, these conditions were kept constant: 400 rpm stirring speed, and 55 : 1 liquid to solid ratio. For process intensification experiments, RVM intensity (%) was varied from 10, 30, 50, and 70 g, and RVM time (minutes) was varied from 1, 12, 20, and 30 minutes.

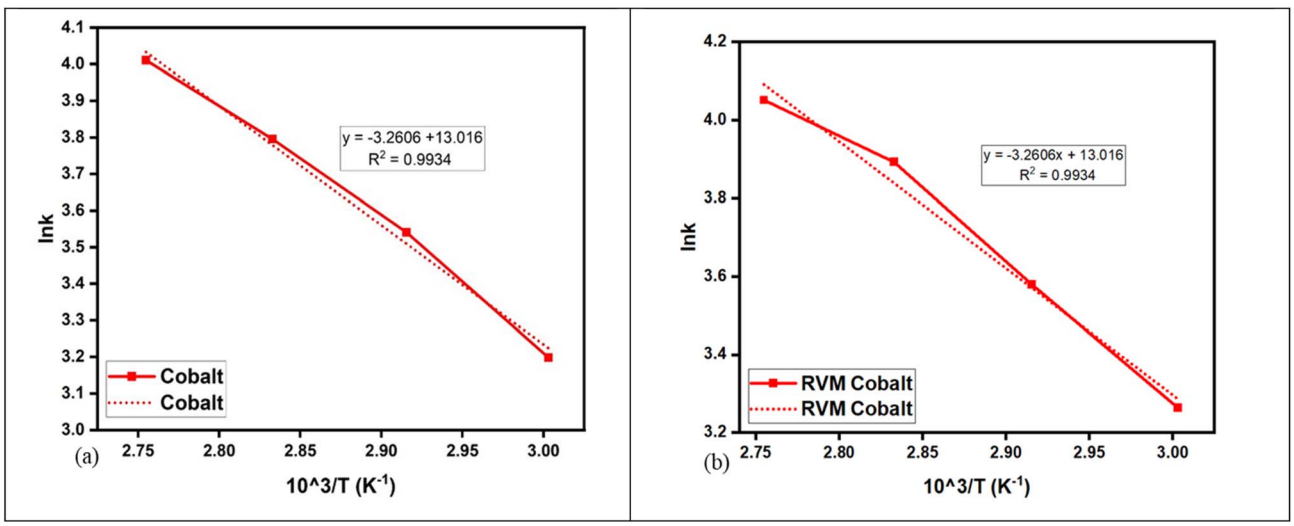


Fig. 6 Arrhenius plots comparison for (a) Co leaching conversion (%) and (b) Co RVM conversion (%).

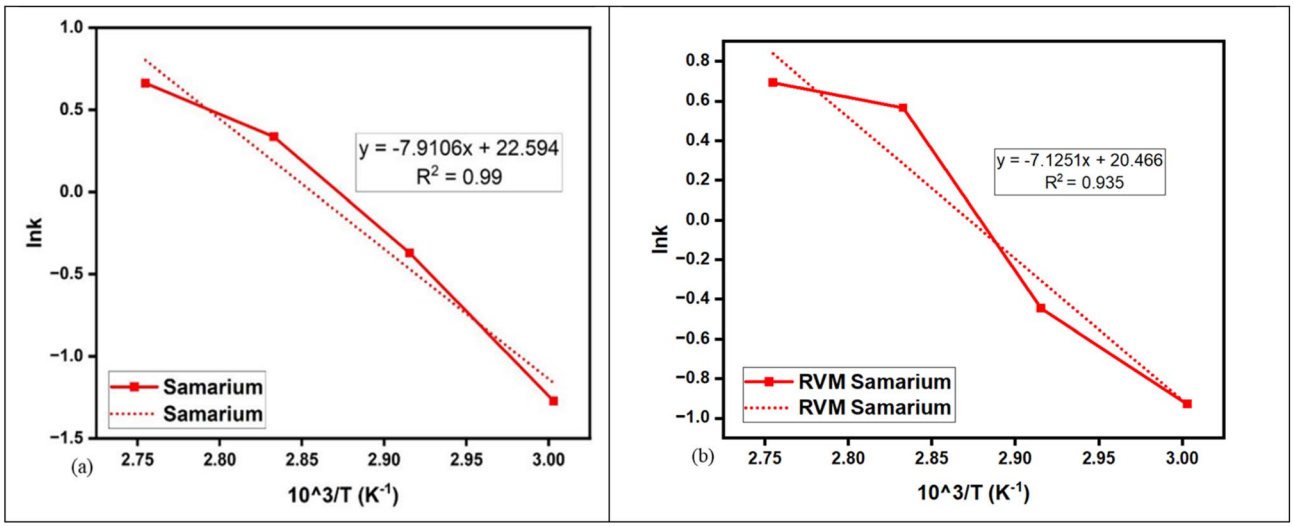


Fig. 7 Comparison of Arrhenius plots for (a) Sm leaching conversion (%) and (b) Sm RVM conversion (%).

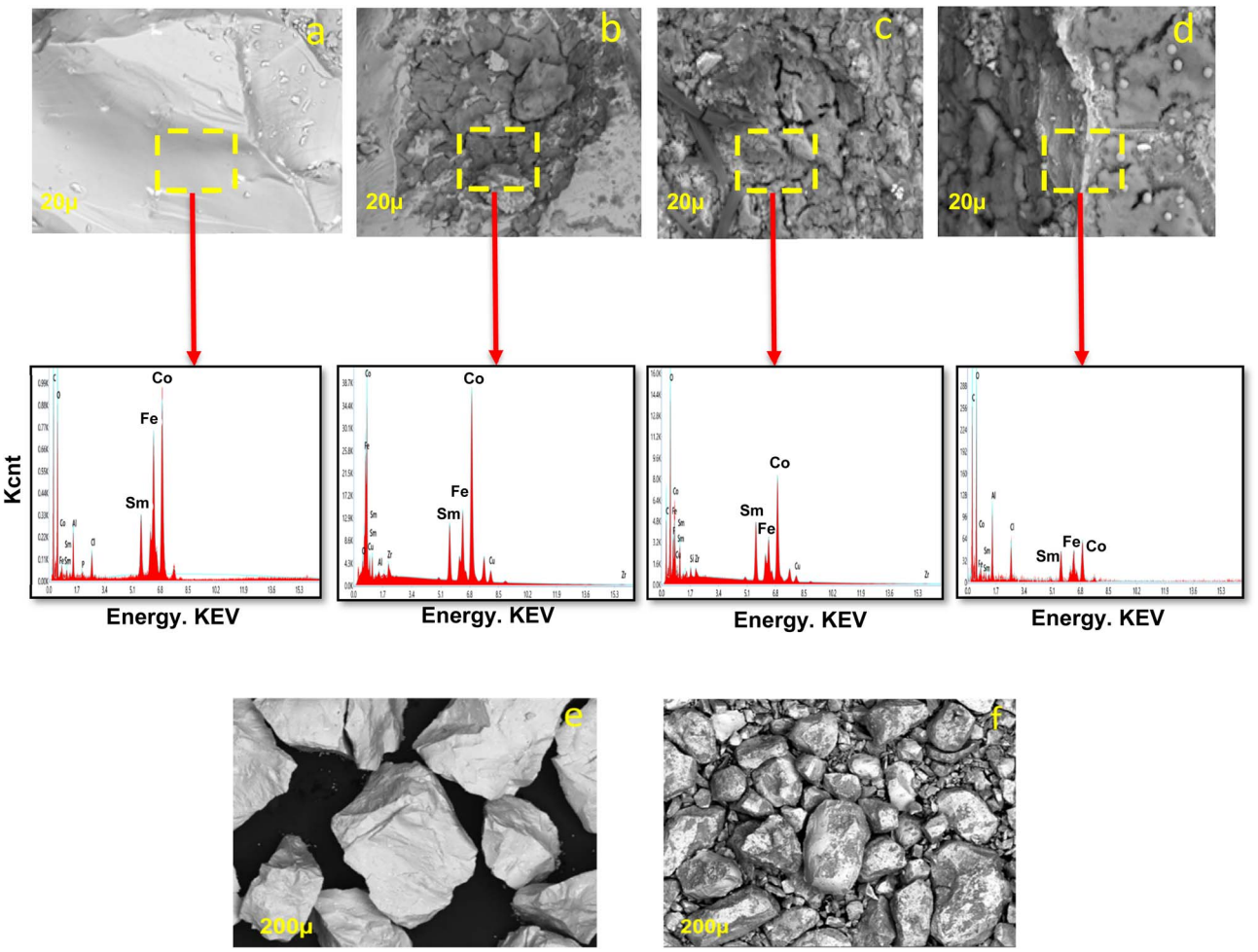


Fig. 8 SEM-EDS images (a–c) of the oxaline leach residue obtained at different leaching times: (a) feed sample, (b) 1 hour, (c) 2 hours, and (d) 5 hours. SEM images corresponding to before leaching (e) and after leaching (f) at 90 °C for 5 hours.

Table 6 The weight (%) determined through EDS analysis for samarium (Sm), cobalt (Co), and iron (Fe) after chemical leaching at 90 °C at 1, 2, 4, and 5 hours using oxaline DES

| | Element | | |
|---|---|---|---|
| Time (hours) | Sm wt (%) | Co wt (%) | Fe wt (%) |
| 1 | 17.1 | 40.1 | 12.2 |
| 2 | 16.9 | 35.5 | 10.7 |
| 4 | 12.1 | 12.2 | 9.6 |
| 5 | 11.6 | 9.6 | 5.5 |

In Fig. 8, as treatment time increases from 1 to 5 hours (1, 2, and 5 h), the SEM pictures clearly show growing surface corrosion and morphological changes, with the initially smooth particle surfaces (image a) becoming rougher and more porous (images b–d). Fe and Co dissolve more readily than Sm, according to EDS spectrum data, which supports the selective character of the oxaline DES leaching process. This selective behaviour is consistent with our conversion measurements, which showed that Sm only converted 5% of the total, whereas Co converted 93.3%. Following 5 hours of leaching, as shown in Table 6, the residual material shows a notable enrichment in Sm content (~11.6%), whilst the concentrations of Co and Fe significantly decrease to 9.6% and 5.5%, respectively. These results show that oxaline DES works as an efficient and selective leaching agent for the preferential recovery of Co from Sm–Co magnetic materials. This could offer an environmentally friendly method for recycling and separating these vital elements from end-of-life magnets.

# 4 Conclusion

This study investigated the effectiveness of DESs as a leaching reagent for extracting Sm and Co from a waste Sm–Co magnet and using RVM for intensifying leaching. Sm and Co's dissolution in DESs was successful and increased over time. RVM increased leaching efficiency by enhancing time-dependent dissolution. Reline, oxaline, and EG–TBAC DESs were selective to Co over Sm. Oxaline with RVM achieved 82% Co recovery under leaching conditions at 80 °C for 2 hours; ethaline showed the lowest Co and highest Sm recovery (14%), indicating DES-specific leaching behaviour.

The preliminary studies showed that oxaline selectively dissolves Co due to a lower activation energy barrier, while Sm requires more energy to break the higher energy barrier. By incorporating higher temperatures for leaching and intensifying conditions, RVM improved Co leaching in oxaline DES to 97% at 90 °C by enhancing mass transfer and reducing boundary resistance without altering reaction kinetics. Sm leaching remained low (maximum 9%) due to strong Sm–O bonds, suggesting a need for pretreatment.

# Author contributions

Zainab Nasrullah: conceptualization, data curation, formal analysis, investigation, methodology, software, validation, visualization, writing – original draft, and writing – review & editing. Frank Agyemang: methodology, data curation, writing – original draft, and writing – review & editing. Mehran Saddat: formal analysis, methodology, and data curation. Richard LaDouceur : supervision, formal analysis, writing – review & editing, funding acquisition, project administration, and resources.

# Conflicts of interest

There are no conflicts of interest to declare.

# Data availability

The data to support the findings of this study are provided in the supplementary information (SI). Supplementary information: additional tables of experimental data from ICP-OES analysis, fit statistics and analysis of variance. See DOI: https://doi.org/10.1039/d5va00283d.

# Acknowledgements

This research was sponsored by the Combat Capabilities Development Command Army Research Laboratory and was accomplished under Cooperative Agreement Number W911NF-22-2-0015. The views and conclusions contained in this document are those of the authors and should not be interpreted as representing the official policies, either expressed or implied, of the Combat Capabilities Development Command Army Research Laboratory or the U.S. government. We would also like to acknowledge Gary Wyss, and Cristina Stefanescu from the Center of Advanced Materials Processing (CAMP) at Montana Technological University for their valuable assistance and support throughout the course of this research.

# References

1 S. Peelman, Z. H. I. Sun, J. Sietsma and Y. Yang, Leaching of Rare Earth Elements: Review of Past and Present Technologies, in *Rare Earths Industry: Technological, Economic, and Environmental Implications*, Elsevier Inc., 2015, pp. 319–334.
2 T. Dutta, K. H. Kim, M. Uchimiya, E. E. Kwon, B. H. Jeon, A. Deep, *et al.*, Global demand for rare earth resources and strategies for green mining, *Environ. Res.*, 2016, **150**, 182–190.
3 H. X. Mai, Y. W. Zhang, R. Si, Z. G. Yan, L. D. Sun, L. P. You, *et al.*, High-quality sodium rare-earth fluoride nanocrystals: controlled synthesis and optical properties, *J. Am. Chem. Soc.*, 2006, **128**(19), 6426–6436, DOI: 10.1021/ja060212h.
4 United States Department of Energy, Critical Materials Rare Earths Supply Chain: A Situational White Paper, 2020, Available from, https://www.energy.gov/eere/amo/articles/critical-materials-supply-chain-white-paper-april-2020.
5 G. Inman, I. C. Nlebedim and D. Prodius, Application of Ionic Liquids for the Recycling and Recovery of Technologically Critical and Valuable Metals, *Energies*, 2022, **15**(2), 628, DOI: 10.3390/en15020628.

6 I. Makarova, E. Soboleva, M. Osipenko, I. Kurilo, M. Laatikainen and E. Repo, Electrochemical leaching of rare-earth elements from spent NdFeB magnets, *Hydrometallurgy*, 2020, **192**, 105264, DOI: 10.1016/j.hydromet.2020.105264.
7 J. Z. Wang, Y. C. Tang and Y. H. Shen, Leaching of Sm, Co, Fe, and Cu from Spent SmCo Magnets Using Organic Acid, *Metals*, 2023, **13**(2), 233, DOI: 10.3390/met13020233.
8 R. Herrington, Mining our green future, *Nat. Rev. Mater.*, 2021, **6**, 456–458, DOI: 10.1038/s41578-021-00325-9.
9 N. T. Nassar and S. M. Fortier, *Methodology and Technical Input for the 2021 Review and Revision of the U.S. Critical Minerals List*, 2021, DOI: 10.3133/ofr20211045.
10 F. J. Alguacil and J. I. Robla, Recent Work on the Recovery of Rare Earths Using Ionic Liquids and Deep Eutectic Solvents, *Minerals*, 2023, **13**, 1288, DOI: 10.3390/min13101288.
11 C. K. Gupta and N. Krishnamurthy, *Extractive Metallurgy of Rare Earths*, CRC Press, 2005, p. 484.
12 X. Li, Z. Li, M. Orefice and K. Binnemans, Metal Recovery from Spent Samarium-Cobalt Magnets Using a Trichloride Ionic Liquid, *ACS Sustain. Chem. Eng.*, 2019, **7**(2), 2578–2584.
13 X. Li, Z. Li, M. Orefice and K. Binnemans, Metal Recovery from Spent Samarium-Cobalt Magnets Using a Trichloride Ionic Liquid, *ACS Sustain. Chem. Eng.*, 2019, **7**(2), 2578–2584.
14 S. S. Foltova, T. V. Hoogerstraete, D. Banerjee and K. Binnemans, Samarium/cobalt separation by solvent extraction with undiluted quaternary ammonium ionic liquids, *Sep. Purif. Technol.*, 2019, **210**, 209–218.
15 H. S. Yoon, C. J. Kim, K. W. Chung, S. Jeon, I. Park, K. Yoo, *et al.*, The Effect of Grinding and Roasting Conditions on the Selective Leaching of Nd and Dy from NdFeB Magnet Scraps, *Metals*, 2015, **5**(3), 1306–1314, available from, https://www.mdpi.com/2075-4701/5/3/1306/htm.
16 P. K. Parhi, T. R. Sethy, P. C. Rout and K. Sarangi, Separation and recovery of neodymium and praseodymium from permanent magnet scrap through the hydrometallurgical route, *Sep. Sci. Technol.*, 2016, **51**(13), 2232–2241, DOI: 10.1080/01496395.2016.1200087.
17 A. Kumari, M. K. Sinha, S. Pramanik and S. K. Sahu, Recovery of rare earths from spent NdFeB magnets of wind turbines: Leaching and kinetic aspects, *Waste Manag.*, 2018, **75**, 486–498, available from, https://pubmed.ncbi.nlm.nih.gov/29397277/.
18 X. Jing, Z. Sun, D. Zhao, H. Sun and J. Ren, Single-Stage Extraction and Separation of $Co^{2+}$ from $Ni^{2+}$ Using Ionic Liquid of [C4H9NH3][Cyanex 272], *Molecules*, 2022, **27**(15), 4806, DOI: 10.3390/molecules27154806.
19 S. Prusty, S. Pradhan and S. Mishra, Extraction and separation studies of Nd/Fe and Sm/Co by deep eutectic solvent containing Aliquat 336 and glycerol, *J. Chem. Technol. Biotechnol.*, 2023, **98**(7), 1631–1641.
20 M. H. Severson, R. T. Nguyen, J. Ormerod, A. Palasyuk and J. Cui, A preliminary feasibility study of potential market applications for non-commercial technology magnets, *Heliyon*, 2022, **8**(12), e11773, DOI: 10.1016/j.heliyon.2022.e11773.
21 J. M. D. Coey, Perspective and Prospects for Rare Earth Permanent Magnets, *Engineering*, 2020, **6**(2), 119–131.
22 E. L. Smith, A. P. Abbott and K. S. Ryder, Deep Eutectic Solvents (DESs) and Their Applications, *Chem. Rev.*, 2014, **114**(21), 11060–11082, DOI: 10.1021/cr300162p.
23 G. R. T. Jenkin, A. Z. M. Al-Bassam, R. C. Harris, A. P. Abbott, D. J. Smith, D. A. Holwell, *et al.*, The application of deep eutectic solvent ionic liquids for environmentally-friendly dissolution and recovery of precious metals, *Miner. Eng.*, 2016, **87**, 18–24.
24 Q. Zhang, K. De Oliveira Vigier, S. Royer and F. Jérôme, Deep eutectic solvents: syntheses, properties and applications, *Chem. Soc. Rev.*, 2012, **41**(21), 7108–7146, available from, https://pubs.rsc.org/en/content/articlehtml/2012/cs/c2cs35178a.
25 F. Agyemang, M. Saddat, Z. Nasrullah and R. LaDouceur, Selective Leaching of Rare Earth Elements from Complex Rare Earth Ore Using Deep Eutectic Solvents, *Metall. Mater. Eng.*, 2025, 5.
26 A. P. Abbott, G. Capper, D. L. Davies, R. K. Rasheed and V. Tambyrajah, Novel solvent properties of choline chloride/urea mixtures, *Chem. Commun.*, 2003, (1), 70–71.
27 A. P. Abbott, G. Capper, D. L. Davies, K. J. McKenzie and S. U. Obi, Solubility of Metal Oxides in Deep Eutectic Solvents Based on Choline Chloride, *J. Chem. Eng. Data*, 2006, **51**, 1280–1282, DOI: 10.1021/je060038c.
28 A. P. Abbott, R. C. Harris and K. S. Ryder, Application of hole theory to define ionic liquids by their transport properties, *J. Phys. Chem. B*, 2007, **111**(18), 4910–4913, available from, https://pubmed.ncbi.nlm.nih.gov/17388488/.
29 Q. Zhang, K. D. O. Vigier, S. Royer and F. Jérôme, Deep eutectic solvents: syntheses, properties and applications, *Chem. Soc. Rev.*, 2012, **41**(21), 7108–7146, available from, https://pubs.rsc.org/en/content/articlehtml/2012/cs/c2cs35178a.
30 E. L. Smith, A. P. Abbott and K. S. Ryder, Deep eutectic solvents (DESs) and their applications, *Chem. Rev.*, 2014, **114**(21), 11060–11082, available from, https://pubmed.ncbi.nlm.nih.gov/25300631/.
31 N. G. Picazo-Rodríguez, M. D. J. Soria-Aguilar, A. Martínez-Luévanos, I. Almaguer-Guzmán, J. Chaidez-Félix and F. R. Carrillo-Pedroza, Direct Acid Leaching of Sphalerite: An Approach Comparative and Kinetics Analysis, *Minerals*, 2020, **10**(4), 359, available from, https://www.mdpi.com/2075-163X/10/4/359/htm.
32 K. Binnemans and P. T. Jones, Ionic Liquids and Deep-Eutectic Solvents in Extractive Metallurgy: Mismatch Between Academic Research and Industrial Applicability, *J. Sustain. Metall.*, 2023, **9**(2), 423–438.
33 A. Jani, T. Sohier and D. Morineau, Phase behavior of aqueous solutions of ethaline deep eutectic solvent, *J. Mol. Liq.*, 2020, **304**, 112701, available from, https://hal.science/hal-02498135.
34 J. G. Osorio and F. J. Muzzio, Evaluation of resonant acoustic mixing performance, *Powder Technol.*, 2015, **278**, 46–56, available from, https://www.researchgate.net/publication/

 

273060697_Evaluation_of_Resonant_Acoustic_Mixing_Performance.
35 *What is ResonantAcoustic® Mixing? – Resodyn Acoustic Mixers*, cited 2024 Jan 4, available from, https://resodynmixers.com/2020/12/30/what-is-resonantacoustic-mixing/.
36 E. Golubina, N. Kizim and N. Alekseeva, Intensification of the extraction of rare earth elements at the local mechanical vibration in the interfacial layer, *Chem. Eng. Process.*, 2018, **132**, 98–104.
37 M. N. Babu, K. K. Sahu and B. D. Pandey, Zinc recovery from sphalerite concentrate by direct oxidative leaching with ammonium, sodium and potassium persulphates, *Hydrometallurgy*, 2002, **64**, 119–129, DOI: 10.1016/S0304-386X(02)00030-0.
38 A. Skulcova, A. Russ, M. Jablonsky and J. Sima, The pH behavior of seventeen deep eutectic solvents, *Bioresources*, 2019, **13**(3), 5042–5051.
39 F. S. Mjalli, J. Naser, B. Jibril, V. Alizadeh and Z. Gano, Tetrabutylammonium chloride based ionic liquid analogues and their physical properties, *J. Chem. Eng. Data*, 2014, **59**(7), 2242–2251, DOI: 10.1021/je5002126.
40 P. Das, B. Behera, K. Sanjay and N. Devi, Solvoleaching approach for SmCo5 alloy scrap and production of sodium samarium sulfate and cobalt oxide, *J. Alloys Compd.*, 2025, **1035**, 181469, available from, https://www.sciencedirect.com/science/article/abs/pii/S0925838825030300.
41 X. Li, Z. Li, M. Orefice and K. Binnemans, Metal Recovery from Spent Samarium-Cobalt Magnets Using a Trichloride Ionic Liquid, *ACS Sustain. Chem. Eng.*, 2019, **7**(2), 2578–2584, DOI: 10.1021/acssuschemeng.8b05604.
42 X. Li, A. Van Den Bossche, T. V. Hoogerstraete and K. Binnemans, Ionic liquids with trichloride anions for oxidative dissolution of metals and alloys, *Chem. Commun.*, 2018, **54**(5), 475–478, available from, https://pubs.rsc.org/en/content/articlehtml/2018/cc/c7cc08645h.
43 F. Ortu, Rare Earth Starting Materials and Methodologies for Synthetic Chemistry, *Chem. Rev.*, 2022, **122**(6), 6040–6116, DOI: 10.1021/acs.chemrev.1c00842.
44 N. Peeters, K. Janssens, D. de Vos, K. Binnemans and S. Riaño, Choline chloride–ethylene glycol based deep-eutectic solvents as lixiviants for cobalt recovery from lithium-ion battery cathode materials: are these solvents really green in high-temperature processes?, *Green Chem.*, 2022, **24**(17), 6685, available from, https://pmc.ncbi.nlm.nih.gov/articles/PMC9426644/.
45 F. J. Alguacil, Utilizing Deep Eutectic Solvents in the Recycle, Recovery, Purification and Miscellaneous Uses of Rare Earth Elements, *Molecules*, 2024, **29**(6), 1356, available from, https://pmc.ncbi.nlm.nih.gov/articles/PMC10974661/.
46 C. Wang, Z. Zhou, X. Zhang, H. Guo and G. Boczkaj, Metal extraction using deep eutectic solvents for metal recovery and environmental remediation – a review, *Sep. Purif. Technol.*, 2025, **364**, 132533, available from, https://www.sciencedirect.com/science/article/abs/pii/S138358662501130X.
47 T. Priamushko, E. Franz, A. Logar, L. Bijelić, P. Guggenberger, D. Escalera-López, *et al.*, Be Aware of Transient Dissolution Processes in Co3O4 Acidic Oxygen Evolution Reaction Electrocatalysts, *J. Am. Chem. Soc.*, 2025, **147**, 3528, DOI: 10.1021/jacs.4c14952.
48 S. Stuurman, S. Ndlovu and V. Sibanda, Comparing the extent of the dissolution of copper-cobalt ores from the DRC Region, *J. South. Afr. Inst. Min. Metall.*, 2014, **114**(4), 00013.
49 T. Lemaoui, F. Abu Hatab, A. S. Darwish, A. Attoui, N. E. H. Hammoudi, G. Almustafa, M. Benaicha, Y. Benguerba and I. M. Alnashef, Molecular-Based Guide to Predict the pH of Eutectic Solvents: Promoting an Efficient Design Approach for New Green Solvents, *ACS Sustainable Chem. Eng.*, 2021, **9**, 5783–5808, DOI: 10.1021/acssuschemeng.0c07367.
50 J. Saien and H. Bamdadi, Mass Transfer from Nanofluid Single Drops in Liquid–Liquid Extraction Process, *Ind. Eng. Chem. Res.*, 2012, **51**(14), 5157–5166, DOI: 10.1021/ie300291k.
51 C. Hanson, *Recent Advances in Liquid-Liquid Extraction*, Pergamon Press Ltd, 1971, pp. 1–585, available from, https://www.sciencedirect.com:5070/book/9780080156828/recent-advances-in-liquid-liquid-extraction.
52 V. Hančil, V. Rod and M. Řeháková, Mass transfer cell with vibrational mixing, *Chem. Eng. J.*, 1978, **16**(1), 51–56.
53 I. N. Perera, G. S. Dobhal, J. M. Pringle, L. A. O'Dell, S. A. Tawfik, T. R. Walsh, *et al.*, A case study using spectroscopy and computational modelling for Co speciation in a deep eutectic solvent, *Phys. Chem. Chem. Phys.*, 2024, **26**(31), 21087–21098.
54 E. Emil-Kaya, X. Lu and B. Friedrich, Recovery of samarium and cobalt/iron oxide from SmCo magnets through acid baking and water leaching, *J. Mater. Cycles Waste Manage.*, 2024, **26**(6), 3905–3916.